

The one pot synthesis of heterobimetallic complexes from a homoditopic pyrimidine–hydrazone ligand†

Daniel J. Hutchinson, Lyall R. Hanton* and Stephen C. Moratti

Cite this: *RSC Adv.*, 2014, 4, 14550

Received 18th December 2013
Accepted 4th March 2014

DOI: 10.1039/c3ra47735e

www.rsc.org/advances

The symmetrical, homoditopic, pyrimidine–hydrazone (pym–hyz) ligand **L1** was used to synthesise three new heterobimetallic complexes, $\text{CuPbL1}(\text{ClO}_4)_4$, $\text{CuAgL1}(\text{SO}_3\text{CF}_3)_3$, and $\text{CuZnL1}(\text{SO}_3\text{CF}_3)_4$. Each of the complexes was produced in a one-pot reaction in CH_3CN , and was isolated in high yield and purity simply by precipitation through the addition of diethyl ether. Analysis was carried out by IR, UV-Vis and ESMS spectroscopy, as well as microanalysis. Crystals were also grown for the purposes of X-ray diffraction studies, which yielded the structures $[\text{CuPbL1}(\text{ClO}_4)(\text{CH}_3\text{CN})_2(\text{H}_2\text{O})](\text{ClO}_4)_3$ (**1**), $[\text{CuAgL1}(\text{SO}_3\text{CF}_3)(\text{CH}_3\text{CN})_2](\text{SO}_3\text{CF}_3)_2 \cdot \text{CH}_3\text{CN}$ (**2**), and $\text{CuZnL1}(\text{SO}_3\text{CF}_3)_2(\text{CH}_3\text{CN})(\text{H}_2\text{O})](\text{SO}_3\text{CF}_3)_2 \cdot \text{CH}_3\text{CN}$ (**3**), all of which were linear complexes containing a Cu(II) ion in one of the pym–hyz–py coordination sites, and either a Pb(II), Ag(I), or Zn(II) ion in the other.

Introduction

The cooperation of two different metal centres imbues heterobimetallic complexes with distinctly different physical and chemical properties from their mono- and homobimetallic analogues.¹ As a result, synthetic heterobimetallics displaying novel properties have been extensively studied and exploited in the fields of catalysis,² mixed spin magnetic systems,³ and molecular sensing and imaging.⁴ Additionally, they act as model compounds for studying the mechanisms and cooperative effects seen in important metalloenzymes which utilise mixed metal ion active sites.⁵

Supramolecular self-assembly can be employed to efficiently synthesise heterobimetallic complexes through the use of ditopic ligands with disparate metal binding sites which are selective towards different metal ions.⁶ The desired heterobimetallic complex can then be achieved by reacting the heteroditopic ligand with the metal ions in a sequential fashion. However, even with carefully designed heteroditopic ligands, these reactions often result in the formation of multiple complexes, necessitating yield limiting purification steps.⁷ Evidently, the synthesis of heterobimetallic complexes is not

trivial and is aided by an adept understanding of molecular recognition.

We have previously reported that the addition of Cu(II) ions to a homoditopic pyrimidine–hydrazone (pym–hyz) ligand (**L1**) in a 1 : 1 metal to ligand ratio resulted in discrete $\text{Cu}(\text{L1H})(\text{ClO}_4)_3$ and $\text{CuL1}(\text{SO}_3\text{CF}_3)_2$ complexes in which one of the coordination sites was occupied by a Cu(II) ion while the other one remained vacant (Fig. 1).⁸ Usually, ditopic pym–hyz ligands self-assemble into $[2 \times 2]$ grids when reacted with Cu(II) ions in a 1 : 1 metal to ligand⁹ ratio as the terpyridine like pym–hyz–py coordination pockets are well suited to binding octahedral metal ions in a coplanar *mer* fashion. However, the addition of hydroxymethyl arms to the terminal py rings of **L1** results in tetradentate coordination to the Cu(II) ion, which prevents the perpendicular arrangement of ligand molecules required to form a grid complex.¹⁰

At the time of publication we envisioned that these monocopper **L1** complexes could be useful precursors in the formation of heterobimetallic complexes.⁸ The facile synthesis of **L1** and the high purity and yield at which the monocopper complexes are synthesised makes them readily accessible. Herein we report that reacting the $\text{Cu}(\text{L1H})(\text{ClO}_4)_3$ and $\text{CuL1}(\text{SO}_3\text{CF}_3)_2$ complexes with either Pb(II), Ag(I) or Zn(II) ions resulted in the formation of heterobimetallic $\text{CuM}^{n+}\text{L1A}_{(2+n)}$ complexes (where A = ClO_4^- or SO_3CF_3^- ; Fig. 2). Each of the complexes was formed in a one pot reaction in which **L1** was first mixed with a solution of Cu(II) ions, before a solution of the other metal ion was added. The heterobimetallic complexes were isolated in high yield without the need for extensive purification steps. They were characterised by microanalysis,

Department of Chemistry, University of Otago, PO Box 56, Dunedin, New Zealand.
E-mail: lhanton@chemistry.otago.ac.nz

† Electronic supplementary information (ESI) available: Crystallographic data for complexes 1–3 including a discussion of how disorder was handled, pictorial views with thermal ellipsoids at the 50% probability level and selected bond lengths and angles in tabulated form. CCDC 976905–976907. For ESI and crystallographic data in CIF or other electronic format see DOI: 10.1039/c3ra47735e



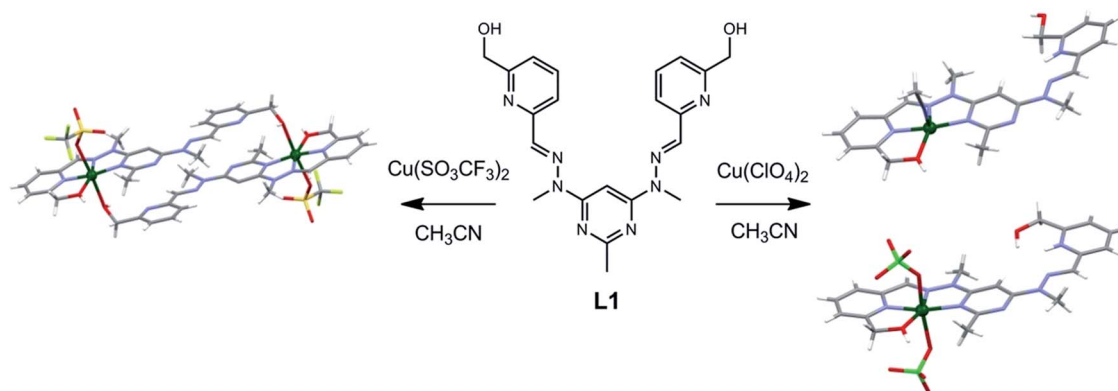


Fig. 1 Solid state structures of the (right) $\text{Cu}(\text{L1H})(\text{ClO}_4)_3$ and (left) $\text{CuL1}(\text{SO}_3\text{CF}_3)_2$ complexes synthesised by reacting **L1** with either $\text{Cu}(\text{ClO}_4)_2$ or $\text{Cu}(\text{SO}_3\text{CF}_3)_2$ in a 1 : 1 metal to ligand ratio.⁸

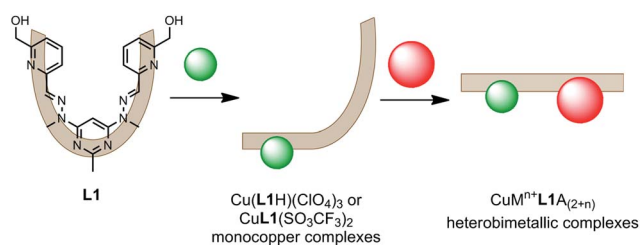


Fig. 2 The two step, one pot synthetic strategy employed to form the heterobimetallic $\text{CuM}^{n+}\text{L1A}_{(2+n)}$ complexes (where $\text{M}^{n+} = \text{Pb}(\text{II}), \text{Ag}(\text{I})$ or $\text{Zn}(\text{II})$, and $\text{A} = \text{ClO}_4^-$ or SO_3CF_3^-).

mass spectrometry, IR and UV-Vis spectroscopy, and X-ray crystallography.

Results

Synthesis and analysis of complexes

The $\text{CuM}^{n+}\text{L1A}_{(2+n)}$ heterobimetallic complexes were all produced in high yields and purity by first synthesising the monocopper $\text{Cu}(\text{L1H})(\text{ClO}_4)_3$ or $\text{CuL1}(\text{SO}_3\text{CF}_3)_2$ complexes, then filling the vacant coordination site with either a $\text{Pb}(\text{II})$, $\text{Ag}(\text{I})$ or $\text{Zn}(\text{II})$ ion (Fig. 2). As previously described, adding a CH_3CN solution of either $\text{Cu}(\text{ClO}_4)_2 \cdot 6\text{H}_2\text{O}$ or $\text{Cu}(\text{SO}_3\text{CF}_3)_2 \cdot 4\text{H}_2\text{O}$ to **L1** in a 1 : 1 metal to ligand ratio resulted in dark green solutions of the monocopper complexes.⁸ Solutions of either $\text{Pb}(\text{ClO}_4)_2 \cdot 3\text{H}_2\text{O}$, AgSO_3CF_3 , or $\text{Zn}(\text{SO}_3\text{CF}_3)_2$ in CH_3CN in a 1 : 1 metal to ligand ratio were then added, and the heterobimetallic complexes were isolated as green precipitates simply by adding diethyl ether to the resulting solutions.

The microanalytical results from the $\text{CuM}^{n+}\text{L1A}_{(2+n)}$ precipitates were consistent with the formulae $\text{CuPbL1}(\text{ClO}_4)_4$, $\text{CuAgL1}(\text{SO}_3\text{CF}_3)_3 \cdot \text{CH}_3\text{CN}$ and $\text{CuZnL1}(\text{SO}_3\text{CF}_3)_4$, while their ESMS spectra showed peaks due to either the $[\text{PbL1-H}]^+$, $[\text{CuAgL1}(\text{SO}_3\text{CF}_3)\text{-H}]^+$, or $[\text{CuL1-H}]^+$ molecular ions, respectively. The IR spectra of the $\text{CuPbL1}(\text{ClO}_4)_4$, $\text{CuAgL1}(\text{SO}_3\text{CF}_3)_3$ and $\text{CuZnL1}(\text{SO}_3\text{CF}_3)_4$ complexes showed an O-H stretching mode at either 3449, 3436 or 3324 cm^{-1} , respectively, which were all typical frequencies of the $\text{Cu}(\text{II})$, $\text{Pb}(\text{II})$, $\text{Ag}(\text{I})$ and $\text{Zn}(\text{II})$

complexes of **L1**.^{8,11,12} The $\text{CuPbL1}(\text{ClO}_4)_4$ and $\text{CuAgL1}(\text{SO}_3\text{CF}_3)_3$ complexes each showed two C=N stretching modes, one of which was at 1565 cm^{-1} , while the other was at either 1541 or 1539 cm^{-1} . The $\text{CuZnL1}(\text{SO}_3\text{CF}_3)_4$ complex showed only the one C=N stretching mode at 1564 cm^{-1} , however it did have a distinct shoulder at 1554 cm^{-1} .

Samples of the complexes were dissolved in CH_3CN and analysed by UV-Vis spectroscopy. Each of the complexes showed a single, broad, featureless d-d transition, in a similar fashion to the mono- and homobimetallic **L1** complexes.⁸ The d-d transitions of the $\text{CuPbL1}(\text{ClO}_4)_4$, $\text{CuAgL1}(\text{SO}_3\text{CF}_3)_3$ and $\text{CuZnL1}(\text{SO}_3\text{CF}_3)_4$ complexes had λ_{max} values of either 697, 670, or 699 nm, and extinction coefficients of either 147, 144, or 135 $\text{L mol}^{-1} \text{cm}^{-1}$, respectively. By comparison the transitions of the mono- and homobimetallic complexes of **L1** had λ_{max} values of 656 nm and 699 nm, respectively, with extinction coefficients of 170 and 250 $\text{L mol}^{-1} \text{cm}^{-1}$, respectively.⁸

X-ray crystallography

Crystals of the $\text{CuM}^{n+}\text{L1A}_{(2+n)}$ complexes were also produced through the diffusion of diethyl ether vapour into the solutions, resulting in the solid state structures of $[\text{CuPbL1}(\text{ClO}_4)(\text{CH}_3\text{CN})_2(\text{H}_2\text{O})](\text{ClO}_4)_3$ (**1**), $[\text{CuAgL1}(\text{SO}_3\text{CF}_3)(\text{CH}_3\text{CN})_2](\text{SO}_3\text{CF}_3)_2 \cdot \text{CH}_3\text{CN}$ (**2**), and $[\text{CuZnL1}(\text{SO}_3\text{CF}_3)_2(\text{CH}_3\text{CN})(\text{H}_2\text{O})](\text{SO}_3\text{CF}_3)_2 \cdot \text{CH}_3\text{CN}$ (**3**; Fig. 3–5). The overall structures of

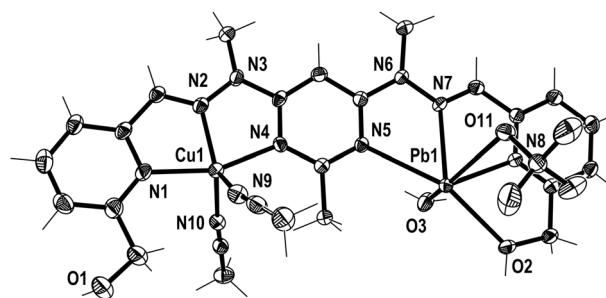


Fig. 3 View of the $[\text{CuPbL1}(\text{ClO}_4)(\text{CH}_3\text{CN})_2(\text{H}_2\text{O})]^{3+}$ cation of complex **1** (crystallographic numbering). Thermal ellipsoids are drawn at the 50% probability level.



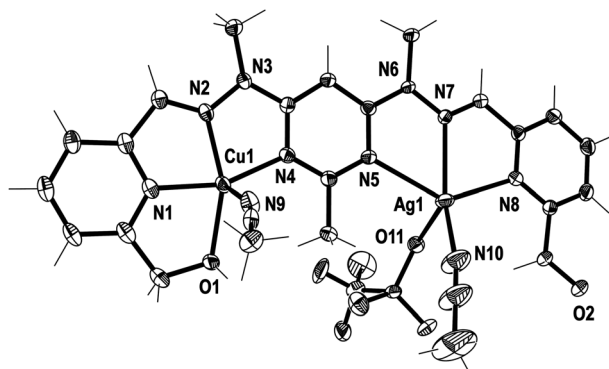


Fig. 4 View of the $[\text{CuAgL1}(\text{SO}_3\text{CF}_3)(\text{CH}_3\text{CN})_2]^{2+}$ cation of complex 2 (crystallographic numbering). Thermal ellipsoids are drawn at the 50% probability level.

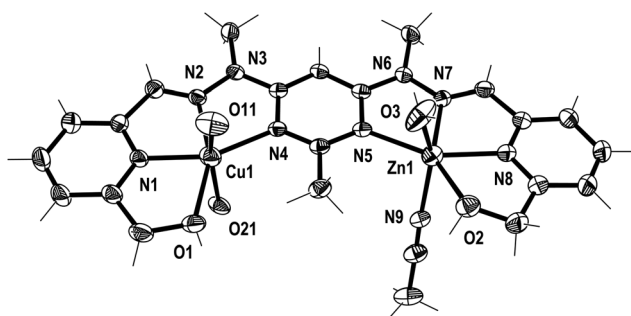


Fig. 5 View of the $[\text{ZnCuZnL1}(\text{SO}_3\text{CF}_3)_2(\text{CH}_3\text{CN})(\text{H}_2\text{O})]^{2+}$ cation of complex 3 (crystallographic numbering). Thermal ellipsoids are drawn at the 50% probability level (the SO_3CF_3^- anions coordinated to Cu1 have been simplified to O11 and O21 for clarity).

these complexes were similar to the previously reported $\text{Cu}_2\text{L1A}_4$, $\text{Pb}_2\text{L1A}_4$, $\text{Ag}_2\text{L1A}_2$ and $\text{Zn}_2\text{L1A}_4$ structures, as well as other pym-hyz ditopic complexes, in that they were linear with both pym-hyz-py bonds in the cisoid-cisoid conformation.^{8,11-13}

Additionally, in complexes 1 and 2, the halves of L1 which were bound to the Cu(II) ions were slightly curved in the mean plane of the central pym ring, while the halves bound to either Pb(II) or Ag(I) were straighter, as seen previously in the homobimetallic L1 complexes.^{8,11,12} As a result the lengths of complexes 1 and 2, 13.45 and 13.19 Å, respectively, were longer than the curved $\text{Cu}_2\text{L1A}_4$ ⁸ complexes but shorter than the straight $\text{Pb}_2\text{L1A}_4$ ¹¹ and $\text{Ag}_2\text{L1A}_2$ ¹² complexes. Both halves of complex 3 were slightly curved in the plane of the central pym ring, resulting in a length of 12.82 Å, which was slightly longer than the $\text{Cu}_2\text{L1A}_4$ complexes and similar in length to the curved $\text{Zn}_2\text{L1}(\text{SO}_3\text{CF}_3)_4$ complex. The intermetallic distances of complexes 1, 2 and 3 were 6.55, 6.36 and 6.11 Å, respectively, which were longer than the Cu-Cu distances previously reported for L1 homobimetallic complexes, but shorter than the Pb-Pb, Ag-Ag and Zn-Zn distances.^{8,11,12}

The crystal structures of the monocopper complexes of L1 all contained a Cu(II) ion bound to the hydroxymethyl arm and N donors of L1 in a tetradentate fashion.⁸ However, when comparing complexes 1-3 it appeared that the tendency of the

hydroxymethyl arm to bind to the Cu(II) ion was controlled by whether the other hydroxymethyl arm was bound to the other metal ion. In complex 1 the Cu(II) ion was not bound to the hydroxymethyl arm, while the Pb(II) ion was, as has been consistently observed in other Pb(II) L1 complexes.¹¹ Conversely, in complex 2 the hydroxymethyl arm was coordinated to the Cu(II) ion, but not to the Ag(I) ion, which commonly does not bind to the hydroxymethyl arms of L1.¹² The asymmetric binding behaviour of the hydroxymethyl arms of L1 was previously observed in the $\text{Cu}_2\text{L1A}_4$ complexes in which only one of the Cu(II) ions in each complex was bound to the hydroxymethyl arms.⁸ In contrast, complex 3 had the hydroxymethyl arms bound to both the Cu(II) and Zn(II) ions.

In addition to the hydroxymethyl arms, each of the metals in 1-3 was bound to the three N donors of the pym-hyz-py sites, CH_3CN solvent molecules, H_2O molecules and either ClO_4^- or SO_3CF_3^- anions. The Cu(II) ions in 1 and 2 adopted either a distorted trigonal bipyramidal ($\tau_5 = 0.59$)¹⁴ or perfect square pyramidal ($\tau_5 = 0.01$)¹⁴ geometry, respectively. The Cu(II) ion in complex 3 had an octahedral geometry which was tetragonally distorted, with elongated bonds to the axially positioned SO_3CF_3^- anions, as is typical of Jahn-Teller distorted octahedral Cu(II) ions.¹⁵ The geometries of the Pb(II) and Zn(II) ions in 1-3 were typical of other Pb(II), and Zn(II) complexes of L1. The Pb(II) ion in 1 adopted a six coordinate geometry, which resembled a distorted pentagonal bipyramid due to the presence of a stereochemically active lone pair of electrons,¹⁶ while the Zn(II) ion in 3 was present in a distorted octahedral geometry. The Ag(I) ion in 2 occupied a distorted square pyramidal environment ($\tau_5 = 0.25$),¹⁴ which is a coordination geometry rarely displayed by Ag(I) ions.¹⁷

Both complexes 1 and 3 displayed H-bonding networks which arranged them into one dimensional chains (Fig. 6 and 7) while complex 2 was H-bonded into dimers (Fig. 8). The $[\text{CuPbL1}(\text{ClO}_4)(\text{CH}_3\text{CN})_2(\text{H}_2\text{O})]^{3+}$ cations of complex 1 were joined by H-bonds between one of the ClO_4^- counterions, and the hydroxymethyl arm, and the ClO_4^- and the H_2O molecule, both of which were bound to the Pb(II) ion. Additionally, there

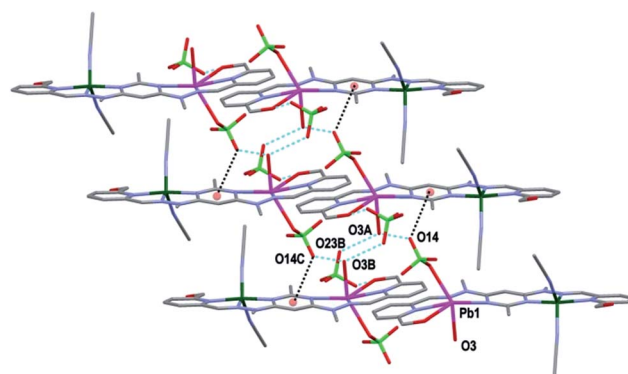


Fig. 6 View of the arrangement of complex 1 into a one dimensional chain in the $[1\ 0\ 0]$ direction through H-bonding. The anion- π interaction between O14 and the central pym rings is also shown (hydrogens have been omitted for clarity; symmetry codes (A) $-1 + x, y, z$; (B) $-x, 1 - y, -z$).



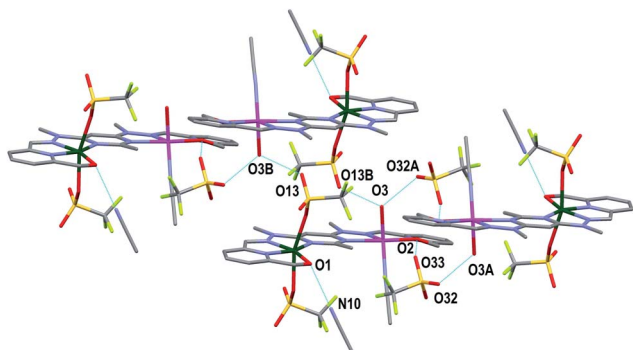


Fig. 7 View of the arrangement of complex **3** into a one dimensional chain in the [1 0 0] direction through H-bonding. The H-bonding interaction between O1 and a CH₃CN molecule is also shown (hydrogens have been omitted for clarity; symmetry codes A: $-x, -y, 1 - z$; B: $1 - x, -y, 1 - z$).

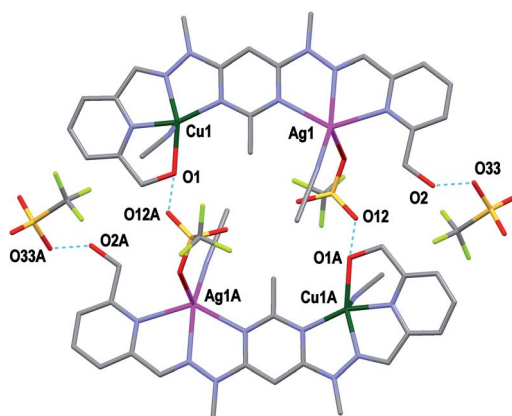


Fig. 8 View of two [CuAgL1(SO₃CF₃)(CH₃CN)₂]²⁺ cations of complex **2** joined as a dimer through H-bonding. Also shown is the H-bonding between O2 and the third SO₃CF₃⁻ anion (symmetry codes A: $2 - x, 1 - y, 1 - z$).

was an intermolecular anion- π interaction¹⁸ in complex **1** between the ClO₄⁻ anion bound to Pb1 and the central pym ring of **L1**. The distance from O14 to the centroid of the pym ring was 3.159(7) Å (Fig. 6). The H-bonding network of complex **3** involved bonds between the H₂O molecules coordinated to Zn(II), the SO₃CF₃⁻ anion bound to Cu(II) in a neighbouring [CuZnL1(SO₃CF₃)₂(CH₃CN)(H₂O)]²⁺ cation, and a free SO₃CF₃⁻ anion which was in turn H-bonded to one of the hydroxymethyl arms of another [CuZnL1(SO₃CF₃)₂(CH₃CN)(H₂O)]²⁺ cation. The other hydroxymethyl arms were H-bonded to a CH₃CN molecule. The [CuAgL1(SO₃CF₃)(CH₃CN)₂]²⁺ cations of complex **2** were paired into dimers by H-bonding between the hydroxymethyl arm coordinated to Cu(II) and the SO₃CF₃⁻ anion coordinated to Ag(I) (Fig. 8).

Experimental

General

All metal salts were purchased from commercial sources and were used as received without further purification with the

exception of Cu(SO₃CF₃)₂·4H₂O, which was produced by the treatment of CuCO₃·Cu(OH)₂·H₂O with aqueous triflic acid. Ligand **L1** was synthesised according to its literature method.⁸ All solvents were used as received, and were of LR grade or better.

Microanalyses were carried out in the Campbell Microanalytical Laboratory, University of Otago. All measured microanalysis results had an uncertainty of ± 0.4 . Electrospray mass spectrometry (ESMS) was carried out on a Bruker microTOFQ instrument (Bruker Daltronics, Bremen, Germany) by employing direct infusion into an ESI source in positive mode. Infrared (IR) spectra were recorded on a Bruker Alpha-P ATR-IR spectrometer. UV-Vis spectra were recorded on an Agilent 8453 spectrophotometer against a CH₃CN background using quartz cells with a 1 cm path length.

CuPbL1(ClO₄)₄

Cu(ClO₄)₂·6H₂O (28.4 mg, 0.0768 mmol) was dissolved in CH₃CN (2.00 mL) and added to a suspension of **L1** (32.0 mg, 0.0762 mmol) in CH₃CN (2.00 mL) stirring at 75 °C. This resulted in complete dissolution of the ligand material and the formation of a clear, green solution. Pb(ClO₄)₂·3H₂O (37.1 mg, 0.0807 mmol) in CH₃CN (2.00 mL) was then added to the stirring solution at 75 °C. The solution was cooled to rt and diethyl ether (20.0 mL) was added, resulting in the precipitation of a green solid. The solid was washed with diethyl ether and dried *in vacuo* (63.9 mg, 78%); Anal. found: C 23.42; H 2.76; N 10.41. Calc. for C₂₁H₂₄N₈O₁₈Cl₄CuPb: C 23.16; H 2.22; N 10.29. ESMS *m/z* found: 627.1653. Calc. for C₂₁H₂₃N₈O₂Pb⁺: 627.1707. Selected IR ν cm⁻¹: 3449br (OH), 3067w (CH), 1600m, 1565m, 1541s (C=N), 1497m, 1431m, 1386w, 1289m, 1269m, 1158m, 1032s (ClO₄⁻). UV-Vis (CH₃CN) λ_{\max} (ϵ)/nm (L mol⁻¹ cm⁻¹): 697 (147). Green crystals suitable for X-ray determination were grown by the slow diffusion of diethyl ether into a CH₃CN solution of Cu(ClO₄)₂·6H₂O, Pb(ClO₄)₂·3H₂O and **L1** in a 1 : 1 : 1 ratio. These crystals gave the structure [CuPbL1(ClO₄)(CH₃CN)₂(H₂O)](ClO₄)₃ (**1**).

CuAgL1(SO₃CF₃)₃

As described for CuPbL1(ClO₄)₄ but with Cu(SO₃CF₃)₂·4H₂O (32.3 mg, 0.0745 mmol), **L1** (29.5 mg, 0.0701 mmol), and AgSO₃CF₃ (20.5 mg, 0.0801 mmol); green solid (58.8 mg, 83%); Anal. found: C 29.12; H 2.69; N 11.50. Calc. for C₂₄H₂₄N₈O₁₁F₉S₃CuAg·CH₃CN: C 28.91; H 2.52; N 11.67. ESMS *m/z* found: 737.9842, 482.1249. Calc. for C₂₁H₂₃N₈O₂-CuAg(SO₃CF₃)⁺: 737.9811. Calc. for C₂₁H₂₃N₈O₂Cu⁺: 482.1240. Selected IR ν cm⁻¹: 3436br (OH), 3068w (CH), 1619m, 1599m, 1565m (C=N), 1539m (C=N), 1485m, 1456m, 1430m, 1384m, 1272s, 1235s (SO₃CF₃⁻), 1220s, 1152s, 1045m, 1023s. UV-Vis (CH₃CN) λ_{\max} (ϵ)/nm (L mol⁻¹ cm⁻¹): 670 (144). Green crystals suitable for X-ray determination were grown by the slow diffusion of diethyl ether into a CH₃CN solution of Cu(SO₃CF₃)₂·4H₂O, AgSO₃CF₃, and **L1** in a 1 : 1 : 1 ratio. These crystals gave the structure [CuAgL1(SO₃CF₃)(CH₃CN)₂](SO₃CF₃)₂·CH₃CN (**2**).



Table 1 Crystallographic data

	1	2	3
Formula	C ₂₅ H ₃₂ Cl ₄ CuN ₁₀ O ₁₉ Pb	C ₃₀ H ₃₃ AgCuF ₉ N ₁₁ O ₁₁ S ₃	C ₂₉ H ₃₂ CuF ₁₂ N ₁₀ O ₂₅ S ₄ Zn
<i>M</i>	1189.16	1162.26	1245.80
Crystal system	Triclinic	Triclinic	Triclinic
Space group	<i>P</i> $\bar{1}$	<i>P</i> $\bar{1}$	<i>P</i> $\bar{1}$
<i>a</i> /Å	8.8553(8)	10.0293(2)	13.2894(2)
<i>b</i> /Å	12.1810(11)	14.0756(2)	13.8254(3)
<i>c</i> /Å	18.5657(16)	16.8259(3)	15.4186(2)
α /°	88.849(4)	70.9120(6)	91.4555(15)
β /°	84.339(4)	87.5816(6)	111.9600(15)
γ /°	76.798(5)	72.0006(6)	115.552(2)
<i>V</i> /Å ³	1940.2(3)	2130.25(7)	2310.61(9)
<i>Z</i>	2	2	2
<i>T</i> / <i>K</i>	90(2)	90(2)	100(2)
μ mm ⁻¹	5.248	1.215	4.028
Reflections collected	25 898	51 464	52 974
Unique reflections (<i>R</i> _{int})	7205 (0.0221)	7879 (0.0295)	9368 (0.0295)
<i>R</i> 1 indices [<i>I</i> > 2 σ (<i>I</i>)]	0.0361	0.0299	0.0601
<i>wR</i> 2 (all data)	0.1069	0.0749	0.1659
Crystal size/mm	0.50 × 0.12 × 0.11	0.51 × 0.46 × 0.35	0.15 × 0.13 × 0.06
Max theta	25.50	25.50	66.49
Goodness of fit	1.095	1.057	1.077

CuZnL1(SO₃CF₃)₄

As described for CuPbL1(ClO₄)₄ but with Cu(SO₃CF₃)₂·4H₂O (32.8 mg, 0.0758 mmol), L1 (31.2 mg, 0.0743 mmol), and Zn(SO₃CF₃)₂ (27.3 mg, 0.0752 mmol); green solid (58.3 mg, 69%): Anal. found: C 26.32; H 2.49; N 9.84. Calc. for C₂₅H₂₄N₈O₁₄F₁₂S₄CuZn: C 26.21; H 2.11; N 9.78. ESMS *m/z* found: 482.1114. Calc. for C₂₁H₂₃N₈O₂Cu⁺: 482.1240. Selected IR ν cm⁻¹: 3324br (OH), 3087w (CH), 1602m, 1564m (C=N), 1489w, 1433w, 1387w, 1365w, 1272s, 1220s (SO₃CF₃⁻), 1155s, 1056m, 1023s. UV-Vis (CH₃CN) λ_{max} (ϵ)/nm (L mol⁻¹ cm⁻¹): 699 (135). Green crystals suitable for X-ray determination were grown by the slow diffusion of diethyl ether into a CH₃CN solution of Cu(SO₃CF₃)₂·4H₂O, Zn(SO₃CF₃)₂, and L1 in a 1 : 1 : 1 ratio. These crystals gave the structure CuZnL1-(SO₃CF₃)₂(CH₃CN)(H₂O)](SO₃CF₃)₂·CH₃CN (3).

X-ray crystallography information

Crystallographic data are summarised in Table 1, while selected bond lengths and angles for complexes 1–3 are available in the supporting information. X-ray diffraction data for complexes 1 and 2 were collected on a Bruker APEX II CCD diffractometer, with graphite monochromated Mo-K α (λ = 0.71073 Å) radiation. Intensities for complexes 1 and 2 were corrected for Lorentz polarisation effects¹⁹ and a multiscan absorption correction²⁰ was applied. The X-ray diffraction data for complex 3 were collected on an Agilent Supernova dual radiation source XRD with an Atlas detector and mirror monochromated Cu (λ = 1.5418 Å) radiation. The data for complex 3 was processed using Agilent CrysAlisPro software (version 1.171.36),²¹ and an analytical absorption correction²² was applied.

The structures of complexes 1–3 were solved by direct methods (SHELXS²³ or SIR-97²⁴) and refined on *F*² using all data

by full-matrix least-squares procedures (SHELXL 97²⁵). All calculations were performed using the WinGX interface.²⁶ Detailed analyses of the extended structure were carried out using PLATON²⁷ and MERCURY²⁸ (Version 2.4).

Conclusions

The heterobimetallic complexes CuPbL1(ClO₄)₄, CuAgL1-(SO₃CF₃)₃, and CuZnL1(SO₃CF₃)₄ were synthesised by reacting the homoditopic ligand, L1, with either Cu(ClO₄)₂·6H₂O or Cu(SO₃CF₃)₂·4H₂O, followed by either Pb(ClO₄)₂·3H₂O, AgSO₃CF₃, or Zn(SO₃CF₃)₂. The reactions were carried out in CH₃CN, in a one pot reaction, and the heterobimetallic complexes were isolated in high yield and purity simply by precipitating them out of solution through the addition of diethyl ether. Crystals of the complexes were also grown through vapour diffusion of diethyl ether. The X-ray diffraction studies of these showed the solid state structure of the complexes were all linear, with a Cu(II) ion in one coordination pocket and either a Pb(II), Ag(I) or Zn(II) ion in the other. The ability of L1 to produce these complexes in high yield and purity from one pot reactions, despite its symmetrical, homoditopic nature, makes it an interesting addition to the array of ligands currently employed to synthesise heterobimetallic complexes.

Acknowledgements

We thank the Department of Chemistry, University of Otago and the New Economic Research Fund of the Foundation for Research, Science and Technology (NERF Grant No UOO-X0808) for financial support.



Notes and references

- 1 (a) B. G. Cooper, J. W. Napoline and C. M. Thomas, *Catal. Rev.: Sci. Eng.*, 2012, **54**, 1–40; (b) D. Astruc, E. Boisselier and C. Ornelas, *Chem. Rev.*, 2010, **110**, 1857–1959; (c) V. Ritleng and M. J. Chetcuti, *Chem. Rev.*, 2007, **107**, 797–858; (d) N. Wheatley and P. Kalck, *Chem. Rev.*, 1999, **99**, 3379–3420; (e) D. W. Stephan, *Coord. Chem. Rev.*, 1989, **95**, 41–107.
- 2 (a) W. Guan, S. Yamabe and S. Sakaki, *Dalton Trans.*, 2013, **42**, 8717–8728; (b) S. Gu, D. Xu and W. Chen, *Dalton Trans.*, 2011, **40**, 1576–1583; (c) A. Zanardi, J. A. Mata and E. Peris, *J. Am. Chem. Soc.*, 2009, **131**, 14531–14537; (d) S. Maggini, *Coord. Chem. Rev.*, 2009, **253**, 1793–1832; (e) A. Fihri, V. Artero, M. Razavet, C. Baffert, W. Leibl and M. Fontecave, *Angew. Chem., Int. Ed.*, 2008, **47**, 564–567.
- 3 (a) S. Öz, J. Titiš, H. Nazir, O. Atakol, R. Boča, I. Svoboda and H. Fuess, *Polyhedron*, 2013, **59**, 1–7; (b) J. Černák, I. Kočanová and M. Orendá, *Comments Inorg. Chem.*, 2012, **33**, 2–54; (c) T. D. Pasatoiu, C. Tiseanu, A. M. Madalan, B. Jurca, C. Buhayon, J. P. Sutter and M. Andruh, *Inorg. Chem.*, 2011, **50**, 5879–5889.
- 4 (a) C.-F. Chow, M. H. W. Lam and W.-Y. Wong, *Anal. Chem.*, 2013, **85**, 8246–8253; (b) A. Boulay, S. Laine, N. Leygue, E. Benosit, S. Laurent, L. V. Elst, R. N. Muller, B. Mestre-Voegtle and C. Picard, *Tetrahedron Lett.*, 2013, **54**, 5395–5398.
- 5 (a) L. M. K. Dassama, A. K. Boal, C. Krebs, A. C. Rosenzweig and J. M. Bollinger, *J. Am. Chem. Soc.*, 2012, **134**, 2520–2523; (b) P. A. Lindahl, *Inorg. Biochem.*, 2012, 172–178; (c) V. R. I. Kaila, M. I. Verkhovsky and M. Wikström, *Chem. Rev.*, 2010, **110**, 7062–7081; (d) W. Jiang, D. Yun, L. Saleh, E. W. Barr, G. Xing, L. M. Hoffart, M. A. Maslak, C. Krebs and J. M. Bollinger, *Science*, 2007, **316**, 1188–1191; (e) J. A. Tainer, E. D. Getzoff, J. S. Richardson and D. C. Richardson, *Nature*, 1983, **306**, 284–287.
- 6 (a) S. K. Goforth, R. C. Walroth and L. McElwee-White, *Inorg. Chem.*, 2013, **52**, 5692–5701; (b) M. R. Halvagar, B. Neisen and W. B. Tolman, *Inorg. Chem.*, 2013, **52**, 793–799; (c) R. Maity, H. Koppetz, A. Hepp and F. E. Hahn, *Inorg. Chem.*, 2013, **135**, 4966–4969; (d) N. Wang, J.-S. Lu, T. M. McCormick and S. Wang, *Dalton Trans.*, 2012, **41**, 5553–5561; (e) Z.-L. You, Y. Lu, N. Zhang, B.-W. Ding, H. Sun, P. Hou and C. Wang, *Polyhedron*, 2011, **30**, 2186–2194; (f) D. Huang and R. H. Holm, *J. Am. Chem. Soc.*, 2010, **132**, 4693–4701; (g) D. L. M. Suess and J. C. Peters, *Chem. Commun.*, 2010, **46**, 6554–6556.
- 7 (a) Y. Sano, A. C. Weitz, J. W. Ziller, M. P. Hendrich and A. S. Borovik, *Inorg. Chem.*, 2013, **52**, 10229–10231; (b) C. Uyeda and J. C. Peters, *Chem. Sci.*, 2013, **4**, 157–163.
- 8 D. J. Hutchinson, L. R. Hanton and S. C. Moratti, *Inorg. Chem.*, 2010, **49**, 5923–5934.
- 9 (a) N. Parizel, J. Ramírez, C. Burg, S. Choua, M. Bernard, S. Gambarelli, V. Maurel, L. BreLOT, J.-M. Lehn, P. Turek and A.-M. Stadler, *Chem. Commun.*, 2011, **47**, 10951–10953; (b) A. R. Stefankiewicz, J. Harrowfield, A. Madalan, K. Rissanen, A. N. Sobolev and J.-M. Lehn, *Dalton Trans.*, 2011, **40**, 12320–12332.
- 10 (a) L. N. Dawe, K. V. Shuvaev and L. K. Thompson, *Chem. Soc. Rev.*, 2009, **38**, 2334–2359; (b) M. Ruben, J. Rojo, F. J. Romero-Salguero, L. H. Uppadine and J.-M. Lehn, *Angew. Chem., Int. Ed.*, 2004, **43**, 3644–3662.
- 11 D. J. Hutchinson, L. R. Hanton and S. C. Moratti, *Inorg. Chem.*, 2011, **50**, 7637–7649.
- 12 D. J. Hutchinson, S. A. Cameron, L. R. Hanton and S. C. Moratti, *Inorg. Chem.*, 2012, **51**, 5070–5081.
- 13 A.-M. Stadler, N. Kyritsakas, R. Graff and J.-M. Lehn, *Chem. –Eur. J.*, 2006, **12**, 4503–4522.
- 14 A. W. Addison, T. N. Rao, J. Reedijk, J. van Rijn and G. C. Verschoor, *Dalton Trans.*, 1984, 1349–1356.
- 15 (a) B. Murphy and B. J. Hathaway, *Coord. Chem. Rev.*, 2009, **243**, 237–262; (b) B. J. Hathaway, in *Comprehensive Coordination Chemistry: The synthesis, reactions, properties & applications of coordination compounds*, ed. G. Wilkinson, R. Gillard and J. A. McCleverty, Pergamon Press, Oxford, 1987, vol. 5, ch. 53, pp. 594–600; (c) H. A. Jahn and E. Teller, *Proc. R. Soc. A*, 1937, **161**, 220–223.
- 16 (a) J. Harrowfield, *Helv. Chim. Acta*, 2005, **88**, 2430–2432; (b) L. Shimoni-Livny, J. P. Glusker and C. W. Bock, *Inorg. Chem.*, 1998, **37**, 1853–1867.
- 17 (a) D. J. Hutchinson, M. P. James, L. R. Hanton and S. C. Moratti, *Inorg. Chem.*, 2014, **53**, 2122–2132; (b) K. Chainok, S. M. Neville, C. M. Forsyth, W. J. Gee, K. S. Murray and S. R. Batten, *CrystEngComm*, 2012, **14**, 3717–3726; (c) A. G. Young and L. R. Hanton, *Coord. Chem. Rev.*, 2008, **252**, 1346–1386.
- 18 (a) T. J. Mooibroek, C. A. Black, P. Gamez and J. Reedijk, *Cryst. Growth Des.*, 2008, **8**, 1082–1093; (b) C. A. Black, L. R. Hanton and M. D. Spicer, *Inorg. Chem.*, 2007, **46**, 3669–3679.
- 19 (a) Z. Otwinowski and W. Minor, in *Processing of X-Ray Diffraction Data Collected in Oscillation Mode, Methods in Enzymology, Molecular Crystallography, Part A*, ed. C. W. Carter and R. M. Sweet, Academic Press, New York, 1997, vol. 276, pp. 307–326; (b) SAINT V4, *Area Detector Control and Integration Software*, Siemens Analytical X-ray Systems Inc., Madison, 1996.
- 20 G. M. Sheldrick, *SADABS, Program for Absorption Correction*, University of Göttingen, Göttingen, Germany, 1997.
- 21 Agilent Technologies, *Xcalibur/Supernova CCD system, CrysAlisPro Software System, version 1.171.36.XX*, 2012, Agilent Technologies UK Ltd, Oxford, UK.
- 22 R. C. Clark and J. S. Reid, *Acta Crystallogr., Sect. A: Found. Crystallogr.*, 1995, **51**, 887–897.
- 23 G. M. Sheldrick, *Acta Crystallogr., Sect. A: Found. Crystallogr.*, 1990, **46**, 467–473.
- 24 A. Altomare, M. C. Burla, M. Camalli, G. L. Casciaro, C. Giacovazzo, A. Guagliardi, A. G. G. Moliterni, G. Polidori and R. Spagna, *J. Appl. Crystallogr.*, 1999, **32**, 115–119.
- 25 G. M. Sheldrick, *SHELXL-97, Program for the Solution of Crystal Structures*, University of Göttingen, Göttingen, Germany, 1997.



- 26 L. J. Farrugia, *J. Appl. Crystallogr.*, 1999, **32**, 837–838.
- 27 A. L. Spek, *Acta Crystallogr., Sect. A: Found. Crystallogr.*, 1990, **46**, 153–165.
- 28 (a) C. F. Macrae, P. R. Edgington, P. McCabe, E. Pidcock, G. P. Shields, R. Taylor, M. Towler and J. van de Streek, *J. Appl. Crystallogr.*, 2006, **39**, 453–457; (b) I. J. Bruno, J. C. Cole, P. R. Edgington, M. K. Kessler, C. F. Macrae, P. McCabe, J. Pearson and R. Taylor, *Acta Crystallogr., Sect. B: Struct. Sci.*, 2002, **58**, 389–397.

